

# First Order Phase Transition Resulting from Finite Inertia in Coupled Oscillator Systems

Hisa-Aki Tanaka and Allan J. Lichtenberg

*Electronics Research Laboratory and Department of Electrical Engineering and Computer Sciences,  
University of California, Berkeley, California 94720*

Shin'ichi Oishi

*Department of Information and Computer Sciences, Waseda University, Tokyo 169, Japan*

(Received 25 October 1996)

We analyze the collective behavior of a set of coupled damped driven pendula with finite (large) inertia, and show that the synchronization of the oscillators exhibits a first order phase transition synchronization onset, substantially different from the second order transition obtained in the case of no inertia. There is hysteresis between two macroscopic states, a weakly and a strongly coherent synchronized state, depending on the coupling and the initial state of the oscillators. A self-consistent theory is shown to determine these cooperative phenomena and to predict the observed numerical data in specific examples. [S0031-9007(97)02614-8]

PACS numbers: 05.45.+b, 02.50.-r, 05.40.+j, 87.10.+e

Coupled limit-cycle oscillators have been explored to model certain nonlinear phenomena such as the synchronous firing of Asian fireflies [1], circadian rhythms, heart beat generation [2], and the Josephson junction arrays [3]. An insight by Kuramoto first made it possible to construct a solvable model (the Kuramoto model), which captures the essence of these coupled limit-cycle oscillators, explicitly showing the connection to second order phase transitions [4]. In the Kuramoto model and some other relevant physical models, the dynamics is reduced to *first order* phase equations on the  $N$  torus formed by the  $N$  limit cycles due to the weak coupling limit. In a uniform globally coupled case with purely sinusoidal nonlinearity, studied by Kuramoto [4], the equations take the following form:

$$\dot{\theta}_i = \Omega_i + \frac{K}{N} \sum_{j=1}^N \sin(\theta_j - \theta_i), \quad i = 1, \dots, N, \quad (1)$$

where  $\theta_i$  and  $\Omega_i$  are, respectively, the instantaneous phase and the natural frequency of the  $i$ th oscillator. Kuramoto transformed this system to a more physically insightful form by introducing a complex order parameter

$$r(t)e^{i\phi(t)} = N^{-1} \sum_j e^{i\theta_j}, \quad (2)$$

where  $r$  measures the coherence and  $\phi$  is the average phase. Furthermore, by assuming that, in the large  $N$  limit,  $r$  and  $\phi$  are stationary, he was able to obtain an analytic solution for  $r$ .

We have used the Kuramoto ansatz (2) to analyze the more general dynamical system [5]

$$m\ddot{\theta}_i + \dot{\theta}_i = \Omega_i + (K/N) \sum_j \sin(\theta_j - \theta_i). \quad (3)$$

In a mechanical analog,  $m\ddot{\theta}_i$ ,  $\dot{\theta}_i$ , and  $\Omega_i$  can be, respectively, interpreted as the inertia, damping, and driving torque in the  $i$ th rotator. We note that the model (3) is a damped, driven version of a coupled Hamiltonian

system [6,7], but the existence of even small damping greatly modifies the steady-state solutions. In this Letter, we focus on the effect of finite (large) inertia on the synchronization, especially the modification of the phase-transition-like onset, that was found for (1), with a generic distribution of the natural frequencies [4].

In our previous study of (3) with nongeneric, uniformly distributed natural frequencies, a discontinuous phase transition between the incoherent and completely coherent states was shown to take place at two distinct coupling strength thresholds  $K_c^{\text{lower}}$  and  $K_c^{\text{upper}}$ , and a good prediction of their values was obtained as a function of  $m$  [5]. However, whether the inertia or the nongeneric distribution caused the discontinuous transition was not clear. Here, we consider a generic unimodal, natural frequency distribution, with extended tails, such as a Gaussian or Lorentzian, to see if the inertia itself is the cause of the discontinuous transition, and to determine the generic collective behavior induced by the inertia. This allows a direct comparison to the results obtained by Kuramoto [4] in which a second order phase-transition-like onset from an incoherent to a (partially) synchronized state was found as  $K$  was increased. We find that a higher order extension of the Kuramoto theory can be used to determine the collective behavior of (3) with large inertia, and that the inclusion of this inertia results in a first order transition with hysteresis in the phase-coherent states.

Figure 1 shows the typical characteristics for finite (large)  $m$  with large  $N$  and the unimodal, symmetric [ $g(\Omega) = g(-\Omega)$ ] distribution, which is obtained from the numerical simulation (plotted with  $\diamond$ ) of (3) for the Lorentzian case, with  $g(\Omega) = d/\pi(\Omega^2 + d^2)$ ,  $d = 1.0$ , and  $m = 0.95, 2.0$ . A fourth order Runge-Kutta scheme with time step 0.1 is employed to solve (3). Theoretical curves (the solid and dashed curves), calculated below, are compared to the numerical results. Several different

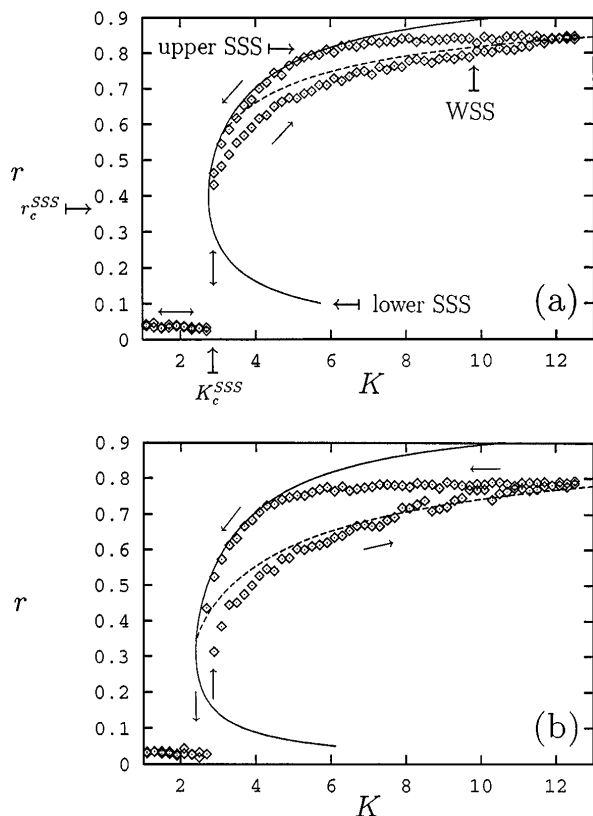


FIG. 1. Hysteretic synchrony observed in Eq. (3) with large inertia. The vertical axis gives the order parameter  $r$  (the degree of the synchrony) of the oscillators; the horizontal axis is the coupling strength  $K$  between the oscillators. Data from numerical simulations of Eq. (3) ( $\diamond$ ) with system size  $N = 500$  and Lorentzian with  $d = 1.0$ ; (a)  $m = 0.95$ , (b)  $m = 2.0$ . Small perturbations to the previous (incoherent) state were introduced;  $\theta_i = 0$  and  $\omega_i = \Omega_i$  for oscillators with  $|\Omega_i| \leq 0.3$ . Curves (solid and dashed) are obtained by the theoretical prediction Eqs. (11) and (12) (see text).

dynamical regimes are observed: an incoherent state (IS), a weakly synchronized state (WSS) (dashed curves), a strongly synchronized state (SSS) (solid curves), and a transition state from the WSS to SSS, as the coupling strength  $K$  is varied up with a small perturbation to the previous  $(\theta_i, \omega_i)$  distribution at each  $K$ , and then down without any perturbation. As  $K$  is increased from small  $K$ , the value of  $r$  persists around the incoherent state [ $r(t) \equiv 0$ ] up to a certain  $K$ . At this point a small fluctuation of  $r(t)$ , which is due to the finite system size  $N$  used in the simulation, triggers a jump to the WSS (the lower branch of the data ( $\diamond$ ) and the dashed curve). The coherence continues to increase as  $K$  is increased. However, if  $K$  is decreased without introducing new  $(\theta_i, \omega_i)$ , the coherence does not follow the original WSS branch but is observed to remain nearly constant until the numerical values join the upper branch of the theory curve, corresponding to the SSS coherence. Beyond this  $K$ , the coherence decreases on the SSS as  $K$  is decreased and finally jumps back to the incoherent state at nearly the same critical  $K$  where the onset of the synchronization

first takes place. Similar numerical results are obtained for a Gaussian distribution.

The theoretical curves for the WSS and SSS are predicted through an extension of the Kuramoto self-consistent theory, to a second order system. We also show these transitions are discontinuous with respect to  $K$ . It should be noted that we approximate a large, but still finite size system (3) by the continuum (infinite size) limit. A specific distribution of  $\Omega$ , the Lorentzian, is considered in the analysis for technical convenience in solving the approximate self-consistent equation. The theory is applicable to other generic distributions such as the Gaussian. We use a coordinate transformation as in (1) to obtain

$$m\ddot{\theta}_i + \dot{\theta}_i = \Omega_i + Kr(t) \sin[\phi(t) - \theta_i], \quad (4)$$

which is a damped driven pendulum with a modulated restoring force and phase modulation. We assume that  $g(\Omega)$  is unimodal, symmetric, and has zero mean. Under these conditions, we seek a particular, self-consistent steady solution  $r(t) \equiv r \geq 0$  and  $\phi(t) \equiv 0$ , i.e., all fluctuations around the steady solution  $r$  vanish as  $N \rightarrow \infty$ , as in the Kuramoto model. In the Kuramoto model, a steady solution ( $r > 0$ ) bifurcates from the IS ( $r \equiv 0$ ) to a partially coherent state at  $K = K_c$  with

$$K_c = 2/\pi g(0), \quad (5)$$

obtained by solving the self-consistent equation for  $r$ .

We have obtained a similar result from the self-consistency of  $r$  for the generalized equations (3) using the following two steps [5]: (i) identify two groups of oscillators that are either locked to the mean phase (2) (denoted by [S]) or mutually incoherent and whirling around the locked group (denoted by [D]), and (ii) measure the contributions from [S] and [D] to the order parameter  $r$ , and equate the sum of them to the original  $r$ . The basic idea of the derivation is the same as Kuramoto's. However, in step (i) care must be taken to consider the initial condition dependence of Eq. (4), since Eq. (4) is a set of damped, driven pendula for a steady state  $r(t) \equiv r$  and  $\phi(t) \equiv 0$ ,

$$m\ddot{\theta} + \dot{\theta} + Kr \sin \theta = \Omega, \quad (6)$$

which has both a stable equilibrium and a whirling limit cycle depending on the parameters [8]. A pendulum starts whirling once the applied torque  $\Omega$  goes beyond a certain threshold  $\Omega_D$ . This  $\Omega_D$  is characterized by the disappearance of the equilibrium point determined by Eq. (6):  $\theta = \sin^{-1}(\Omega/Kr) = \pm\pi/2$ . Then  $\Omega_D(>0)$  is given by  $\Omega_D = Kr$ . On the other hand, below  $\Omega_D$  Eq. (6) can be bistable [8]. The frequency average  $\bar{\Omega} \equiv \langle \dot{\theta} \rangle$  of the whirling solution in Eq. (6) tends to 0 at some  $\Omega_P$  as  $[\ln(\Omega - \Omega_P)]^{-1}$ , resulting in an extremely steep drop of the drifting frequency at  $\Omega_P$  [9].

Consider two particular configurations of the oscillators corresponding to the WSS and SSS, respectively; (I) the increasing  $K$  case, starting from the incoherent state,

and (II) the decreasing  $K$  case starting from the highly coherent state with an arbitrary large  $K$ . In both cases, we start by assuming that the two groups [S] and [D] have certain coherence  $r_{\text{lock}}(\geq 0)$  and  $r_{\text{drift}}(\leq 0)$ , respectively. In case (I), suppose a certain  $r(t) > 0$  is given at any moment, then  $r(t)$  determines the pinning threshold  $\Omega_P$  and the initially drifting oscillators with  $\Omega < \Omega_P$  can be entrained to the locked oscillators [S] after a transient. Thus, it is reasonable to assume that [S] and [D] can be separated at  $\Omega = \Omega_P$  in the natural frequency distribution. On the other hand, in case (II) initially locked oscillators are desynchronized and fall into the drifting state [D] once  $\Omega$  exceeds  $\Omega_D (= Kr)$ . Hence, [S] and [D] can be assumed to be separated at the depinning frequency  $\Omega = \Omega_D$ . From [S], for case (II), as in the Kuramoto model,

$$r_{\text{lock}}^{\text{II}} = Kr \int_{-\pi/2}^{\pi/2} \cos^2 \theta g(Kr \sin \theta) d\theta. \quad (7)$$

For case (I), oscillators with  $\Omega > \Omega_P$  are still drifting on the unit circle and the coherence of the locked oscillators takes the same form as Eq. (7) with  $\pi/2$  being replaced with  $\theta_P = \sin^{-1}[\Omega_P/(Kr)]$ . ( $\theta_P \leq \pi/2$  follows from  $\Omega_P \leq \Omega_D = Kr$ .) From [D]; cases (I) and (II) can be conveniently combined by noting each oscillator is drifting independently of the others as in the Kuramoto model. Then,  $r_{\text{drift}}^{\text{I,II}}$  has the same form as in Kuramoto's analysis;

$$r_{\text{drift}}^{\text{I,II}} = \int_{|\Omega| > \Omega_{P,D}} \oint e^{i\theta} n_D(\theta, \Omega) g(\Omega) d\theta d\Omega, \quad (8)$$

where  $n_D(\theta, \Omega)$  is the density of the desynchronized oscillators [D] with phase  $\theta$  and given driving frequency

$\Omega$ . As  $n_D(\theta, \Omega)$  is proportional to  $|\dot{\theta}|^{-1}$  and  $g(\Omega)$  is symmetric, Eq. (8) can be simplified as

$$r_{\text{drift}}^{\text{I,II}} = \frac{1}{\pi} \int_{\Omega > \Omega_{P,D}} \int_0^{\tilde{T}} \cos \theta(t, \Omega) |\tilde{\Omega}| g(\Omega) dt d\Omega. \quad (9)$$

The self-consistent equation of the steady state  $r(t) \equiv r$  is then

$$r = r_{\text{lock}}^{\text{I,II}} + r_{\text{drift}}^{\text{I,II}}, \quad (10)$$

for cases (I) and (II), respectively.

In our previous work we used a uniform, bounded intrinsic frequency distribution such that  $r_{\text{drift}} \equiv 0$  in the coherent state. This resulted in certain nongeneric features of our solutions, such as separate pinning and depinning critical coupling  $K$ . Here, we are interested in a generic distribution  $g(\Omega)$  with extended tails, which can be compared directly to a similar distribution in Kuramoto's analysis [4]. Taking  $g(\Omega)$  to be Lorentzian we can solve (10) analytically. The first step is to approximate the whirling solution  $\theta(t)$  and  $\tilde{\Omega}$ . This can be done by choosing a small parameter  $(mK)^{-1} \equiv \delta$  and applying the Poincaré-Lindstead method. The second step is the approximation of  $\Omega_P$  by the Melnikov method. This can be done nicely due to the characteristics of Eq. (6) with large  $m$  [9]. Applying these analytic approximations to (10), we find that the lowest order term in (9), after expanding in a series of  $\Delta \equiv (m\Omega)^{-1} \ll 1$ , becomes dominant. After discarding the higher order terms of  $\Delta$  (for details of the method, see [5]), we have the following set of self-consistent equations for cases (I) and (II), respectively.

Case I:

$$r = r_{\text{lock}}^{\text{I}} + r_{\text{drift}}^{\text{I}} = \frac{Kr}{m^2} \left( \frac{1}{\pi d^3} \ln \frac{\sqrt{d^2 + \Omega_P^2}}{\Omega_P} - \frac{1}{2\pi d \Omega_P^2} \right) + \frac{2}{\pi Kr} \left[ \sqrt{d^2 + K^2 r^2} \tan^{-1} \left( \sqrt{d^2 + K^2 r^2} \tan \theta_P \right) - d \theta_P \right],$$

with

$$\theta_P = \sin^{-1}[\Omega_P/(Kr)], \quad \text{and} \quad \Omega_P = (4/\pi) \sqrt{Kr/m}, \quad (11)$$

Case II:

$$r = r_{\text{lock}}^{\text{II}} + r_{\text{drift}}^{\text{II}} = \frac{Kr}{m^2} \left( \frac{1}{\pi d^3} \ln \frac{\sqrt{d^2 + K^2 r^2}}{Kr} - \frac{1}{2\pi d K^2 r^2} \right) + \left( \sqrt{d^2 + K^2 r^2} - d \right) / (Kr). \quad (12)$$

The self-consistent equations for  $r$  (11) and (12) can be numerically solved to obtain the solid and dashed curves in Fig. 1. Since  $Kr$  appears everywhere on the right-hand side of (11) and (12), the simplest procedure is to analyze the graph of  $r(x)$  with  $x \equiv Kr$  and extract  $r = x/K$  (see

[10] for a similar analysis). The results yield the following properties.

(i) In case (I) there is a threshold  $K_c^{\text{SSS}} > K_c$ , which can be obtained analytically for any finite (large)  $m$  and  $d$  as a function of  $m$  and  $d$ . For  $K < K_c^{\text{SSS}}$ , there is no solution for  $r$  except for the trivial IS ( $r \equiv 0$ ). For  $K > K_c^{\text{SSS}}$ , there are two solution branches of  $r$  bifurcating at  $K = K_c^{\text{SSS}}$  into upper increasing  $r$  and lower decreasing  $r$  branches, as shown in Fig. 1. They tend to  $r = 1$  and  $r = 0$ , respectively, as  $K \rightarrow \infty$  and coalesce to  $r \equiv r_c^{\text{SSS}} \sim O(1)$  at  $K = K_c^{\text{SSS}}$ . Thus,  $r(K)$  has a discontinuous jump to the IS at  $K_c^{\text{SSS}}$  as  $K$  is decreased.

(ii) In case (II) there is an increasing branch of  $r$  (WSS) with respect to  $K$  which tends to  $r = 1$  as  $K \rightarrow \infty$ . The other end point of the WSS branch is on the SSS as shown in Fig. 1, which corresponds to  $\theta_P = \pi/2$ . This branch is always below the upper branch in case (I) for all  $K$ .

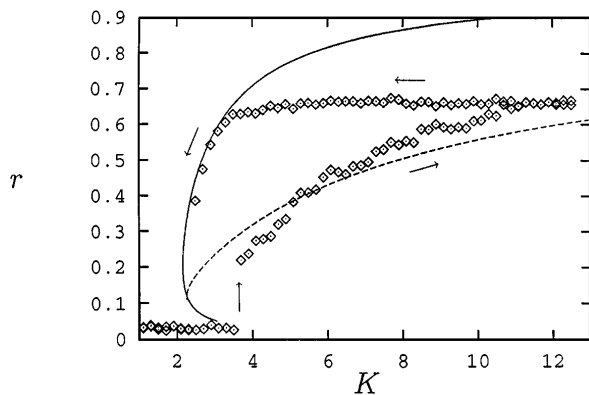


FIG. 2. Coherent branches for at  $m = 6.0$ . Data were obtained in the same conditions as used in Fig. 1. The coherence  $r$  shown is averaged over time after a transient.

As we see in Fig. 1 data from the numerical simulation of (3) and theoretical prediction from (11) and (12) show agreement in the discontinuous jumps and shape of the coherent branch. The (flat) transition from the WSS to SSS can also be understood from the bistability in (6) and the fact that  $\Omega_{P,D}$  decrease as  $K$  decreases; once oscillators are locked to the mean phase, they maintain  $r_{\text{lock}}$  until their  $\Omega_i$  go beyond  $\Omega_D$ .

The approximations in (11) and (12) are not necessarily good approximations to (10) as  $Kr \rightarrow 0$ . However, as we observe in Fig. 1(a), the good agreement between the theoretical and numerical data indicates that the transition takes place in a valid range of  $Kr$  for the approximation. On the other hand, the end point of the lower SSS branch is not captured properly for the above reason. Does some (finite)  $K$  exist where the lower SSS branch touches the IS ( $r \equiv 0$ ) and does a lower branch of WSS exist? Our theory does not provide any stability properties in the self-consistent static state, although, using a special simulation protocol from [11], beyond certain  $K$  the IS is confirmed to be unstable. The predicted lower SSS branch has never been accessible from the IS in the simulation.

For larger  $m$ , although the decreasing SSS branch shows good agreement to the theoretical prediction, the WSS branch shows a growing deviation from the theoretical prediction as seen in Fig. 2. This deviation from the theoretical WSS curve becomes significant for  $m > 3.0$ . To consider the reason for this, we measured the error rate of the experimentally obtained mean frequency over the whirling oscillators to the theoretically calculated one: 6.4%, 7.1%, 11.2% for  $m = 0.95, 2.0, 6.0$  with  $K = 8.0$  and  $N = 500$ , and 2.9%, 4.2%, 10.9% for  $N = 2500$ , respectively. On the other hand, the error rate of the actual  $\Omega_P$  from the theoretical one is reasonable in the above examples: 3.6%, 1.6%, 0.4% for  $m = 0.95, 2.0, 6.0$ , respectively. Thus, the deviation is due to the break of the independence between the whirling oscillators, and it is observed that a secondary synchronization of groups of the whirling oscillators with lower natural frequencies becomes significant for larger  $m$ , as seen in Fig. 3.

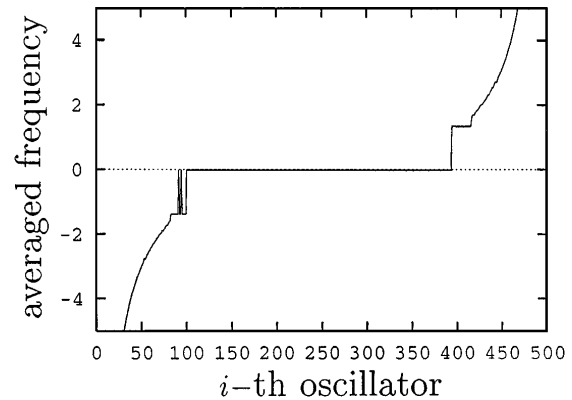


FIG. 3. Numerically determined averaged frequencies  $\langle \dot{\theta} \rangle$  (solid line) for  $i = 1, \dots, 500$ , with  $m = 6.0$  and  $K = 10.2$ , showing the mutual entrainment of whirling oscillators (around  $i = 100$  and 400). The phases  $102 \leq i \leq 395$  are locked, while the other phases are whirling.  $\Omega_i = d \tan[\frac{\pi}{2}(2i - N - 1)/(N + 1)]$  is used to approximate a Lorentzian.

Our results indicate an important difference between the collective behavior of coupled second order equations, and the collective behavior of first order equations analyzed by Kuramoto [4]. The second order generalized Kuramoto system exhibits a first order phase transition [12], with discontinuous jumps and hysteresis, in contrast to a second order phase transition found in the first order (original) Kuramoto system.

We thank M.A. Lieberman, M.D.S. Vieira, S.H. Strogatz, and K. Wiesenfeld for helpful comments, and S. Nii for pointing out the synchronization of the whirling oscillators. Great thanks go to G.B. Ermentrout for a useful note on second order phase equations, and S. Watanabe for helpful discussions throughout the year.

- 
- [1] G. B. Ermentrout, *J. Math. Biol.* **29**, 571 (1991).
  - [2] A. T. Winfree, *The Geometry of Biological Time* (Springer, New York, 1980).
  - [3] K. Wiesenfeld, P. Colet, and S. H. Strogatz, *Phys. Rev. Lett.* **76**, 404 (1996).
  - [4] Y. Kuramoto, *Lecture Notes in Physics* (Springer-Verlag, Berlin, 1975), Vol. 39; *Chemical Oscillations, Waves, and Turbulence* (Springer-Verlag, Berlin, 1984).
  - [5] H. Tanaka, A. J. Lichtenberg, and S. Oishi, *Physica D* (Amsterdam) (to be published).
  - [6] S. Inagaki, *Prog. Theor. Phys.* **90**, 577 (1993).
  - [7] M. Antoni and S. Ruffo, *Phys. Rev. E* **52**, 2361 (1995).
  - [8] M. Levi, F. C. Hoppensteadt, and W. L. Miranker, *Q. Appl. Math.* **36**, 167 (1978).
  - [9] S. H. Strogatz, *Nonlinear Dynamics and Chaos* (Addison-Wesley, Reading, MA, 1994), p. 273.
  - [10] S. H. Strogatz, C. M. Marcus, R. E. Mirollo, and R. M. Westervelt, *Physica (Amsterdam)* **36D**, 23 (1989).
  - [11] S. H. Strogatz and R. E. Mirollo, *J. Stat. Phys.* **63**, 613 (1991).
  - [12] K. Binder, *Rep. Prog. Phys.* **50**, 783 (1987).